Altered membrane trafficking in activated bone marrow-derived macrophages

Albert W. Tsang, Kirsten Oestergaard, Jesse T. Myers, and Joel A. Swanson

Department of Microbiology and Immunology, University of Michigan Medical School, Ann Arbor, Michigan

Abstract: Activation of macrophages with interferon-γ (IFN-γ) and lipopolysaccharide (LPS) leads to increased intracellular resistance to microbes and increased major histocompatibility complex class II-restricted antigen presentation, processes that both use the vacuolar compartment. Despite the requirement of the macrophage vacuolar compartment for microbicidal activities and antigen processing, the rates of endocytosis and membrane trafficking in activated macrophages are not clearly defined. In this study, vacuolar compartment dynamics were analyzed in murine bone marrow-derived macrophages activated with LPS and/or IFN-γ, conditions that increased macrophage nitric oxide production and resistance to infection by *Listeria monocytogenes*. Relative to nonactivated cells, activated macrophages showed diminished rates of fluid-phase pinocytosis and phagocytosis and delayed progression of macropinosomes and phagosomes to late endosomes and lysosomes. In contrast to the slowing of membrane trafficking, rates of macropinosome acidification were similar between activated and nonactivated cells. One consequence of this slowed membrane trafficking in activated macrophages was a prolonged exposure of incoming molecules to an acidic nonlysosomal compartment, a condition which may facilitate microbicidal chemistries or antigen processing. *J. Leukoc. Biol.* 68: 487–494; 2000.

Key Words: *macrophages · activation · Listeria monocytogenes · lipopolysaccharide · interferon-γ · lysosome*

INTRODUCTION

The vacuolar compartment of macrophages, which consists of pinosomes, phagosomes, endosomes, and lysosomes, serves a variety of functions central to this cell's roles in host defense. Delivery of microorganisms by phagocytosis into the macrophage vacuolar compartment is a common prerequisite for killing [1]. Phagolysosomes are generally acidic and hydrolase-rich, and their acidity may facilitate the actions of reactive oxygen or nitrogen species [2]. Antigen processing and presentation via major histocompatibility complex (MHC) class II molecules occur by endocytosis, proteolytic degradation in acidic endocytic compartments, and recycling of antigen-associated membrane proteins to the cell surface [3]. These processes are maintained by high constitutive rates of fluid-phase pinocytosis, membrane recycling, and vesicle fusion with lysosomes [4].

Activating macrophages increases their destructive potential. Macrophages obtained from mice previously exposed to sublethal doses of *Listeria monocytogenes* can kill bacteria more effectively than macrophages from unexposed mice [5]. Macrophage activation results primarily from exposure of macrophages to interferon-γ (IFN-γ) and bacterial products, such as lipopolysaccharide (LPS) or lipoteichoic acid [6, 7]. The enhanced ability to kill microorganisms is largely a result of increased macrophage production of superoxide, nitric oxide, and their derivatives [8]. Although lysosomes and lysosomal enzymes increase in number [9], it is not known if the lysosomes in activated macrophages are more acidic or in some other way more cytotoxic. Resistance to *L. monocytogenes* exhibited by IFN-γ treatment of peritoneal macrophages is evidently because of blockage of escape from the phagosome [10]. Because escape typically occurs within minutes of phagocytosis [11], the mechanism of resistance must reside in the earliest compartments of endocytosis.

Activation-related changes in vacuolar compartment functions may also change the dynamics of those compartments. There is precedent for this in the differentiation of dendritic cells. Undifferentiated dendritic cells exhibit high rates of pinocytosis, and their differentiation into antigen-presenting cells, stimulated by tumor necrosis factor α, interleukin-1β, or LPS, is accompanied by a dramatic and irreversible decrease in pinocytosis [12]. It is not known if, upon activation, macrophages undergo similar alterations in constitutive endocytosis. Early studies indicated that activation increased rates of pinocytosis. Edelson et al. [13] reported high rates of pinocytosis in thioglycollate-elicited mouse macrophages, and Knight et al. [14] observed an immediate stimulation of pinocytosis in bone marrow-derived macrophages exposed to LPS. In contrast, Montaner et al. [15] found reduced rates of fluid-phase pinocytosis in human monocyte-derived macrophages cultured in IFN-γ. Thus, it is not clear whether activation increases or decreases rates of membrane trafficking in macrophages.

Correspondence: Joel A. Swanson, Department of Microbiology and Immunology, University of Michigan Medical School, Ann Arbor, MI 48109-0620. E-mail: jswan@umich.edu

Received January 23, 2000; revised March 27, 2000; accepted April 10, 2000

The confused picture may result in part from differences between experimental systems for studying activation. It is widely acknowledged that there is no single differentiation state called activation; rather, different stimuli will lead to different pathways of differentiation, which are collectively referred to as activation [16]. Macrophages from different sources respond differently to activating stimuli, and a given kind of macrophage will exhibit different profiles of activation responses, depending on the nature of the activation stimulus. Our operational definition of an activated macrophage in this study was one with increased resistance to infection by *L. monocytogenes*, together with increased production of reactive nitrogen intermediates.

We hypothesize that the activated macrophage localizes its most potent antimicrobial effects to phagosomes before they meet lysosomes, either by creating novel compartments or by modifying the dynamics of existing compartments. To define changes in membrane trafficking that distinguish activated cells, we examined bone marrow-derived macrophages activated with IFN-γ and LPS. After confirming that these cells increased production of nitric oxide and resistance to *L. monocytogenes* infection, we measured several features of organelle trafficking. We provide evidence for a slowing of endocytosis and membrane trafficking that allows a brief persistence of endocytosed molecules in acidic nonlysosomal compartments.

MATERIALS AND METHODS

Cells

Bone marrow-derived macrophages were obtained from femurs and tibias of female BALB/c mice (Harlan Sprague-Dawley, Indianapolis, IN) and were cultured for 6–8 days as described earlier [17]. Cells were plated on 13-mm coverslips in 24-well plates or 25-mm coverslips in 6-well plates containing DMEM, 10% heat-inactivated fetal bovine serum, 100 U/ml penicillin, and 100 μg/ml streptomycin (DME-10F; GIBCO BRL, Gaithersburg, MD). Experimental treatments included 100 U/ml recombinant mouse IFN-γ (Genzyme, Cambridge, MA) and 10–1,000 ng/ml LPS (List Biological, Campbell, CA) added to cells for 18–24 h. Washed sheep erythrocytes (sRBC, Reproductive Sciences Program, University of Michigan, Ann Arbor, MI) were opsonized for 45 min at 37°C using rabbit anti-sheep erythrocyte IgG (ICN Biomedical, Aurora, OH), then were washed with phosphate-buffered saline (PBS).

Measurement of nitrite in macrophages

Nitrite production by macrophages was measured using the Griess assay, performed as described by Granger et al. [18]. Briefly, after 24 h incubation of 1.0×10^5 cells in 0.75 ml DME-10F, plus or minus treatments, 0.7 ml cell supernatant was removed and incubated with 0.7 ml Griess reagent (0.05% napthylethylenediamine-HCl + 0.5% sulfanilamide in 1.25% H_3PO_4) for 5 min. Absorbance was measured at 546 nm in a LKB Ultrospec II (Cambridge, England). Standard curves were prepared using $NaNO_2$ in DME-10F.

Measurement of *Listeria monocytogenes* growth in macrophages

The ability of macrophages to kill *L. monocytogenes* was assessed using the method of Jones and Portnoy [19]. After overnight growth at room temperature in brain-heart infusion broth (BHI; Difco, Detroit, MI), *L. monocytogenes* strain 10403S was diluted and further grown for ~1 h to 0.500 $O.D^{600nm}$. After overnight treatment of 2.0×10^5 macrophages per well in 24-well plates, cells were washed 3× in Ringers buffer (RB; 155 mM NaCl, 5mM KCl, 2 mM $CaCl_2$, 1 mM $MgCl_2$, 2 mM NaH_2PO_4, 10 mM Hepes, and 10 mM glucose, pH 7.2), then incubated for 1 h in DME-10F without antibiotics. After incubation, cells were incubated 30 min in 0.5 ml antibiotic-free DME-10F plus bacteria. Infections were designed such that ~5% of the macrophages were infected with *L. monocytogenes* at the earliest measured time point; this required that twice as many bacteria be added to the activated macrophages (3×10^5 bacteria for control cells and 6×10^5 bacteria for IFN-γ and LPS-treated cells; multiplicity of infection of 1.5 and 3, respectively). After infection, cells were washed 4× in warm RB, then incubated 0–5.5 h in DME-10F with 50 μg/ml gentamicin. Cells were then washed 4× in warm RB and lysed in sterile deionized water. Bacteria were then diluted and plated onto bovine heart infusion agar for determination of colony-forming units.

To determine the relationship between inducible nitric oxide synthase (iNOS) expression, F-actin, and *L. monocytogenes*, macrophages on 13-mm coverslips were incubated overnight, with or without treatments. Cells were washed 3× in RB, then incubated in DME-10F without antibiotics for 1 h and infected as described above. They were then fixed 20 min with cytoskeletal fixative (40 mM HEPES, 10 mM EGTA, 0.5 mM EDTA, 5 mM $MgSO_4$, 33 mM potassium acetate, 0.02% sodium azide, 5% polyethylene glycol 400, 4% paraformaldehyde). Cells were then washed 3× with PBS and permeabilized with 0.3% Triton X-100 in PBS for 5 min. Permeabilized cells were washed 3× for 5 min each, then incubated with mouse anti-iNOS (250 ng/ml) (Transduction, Lexington, KY) in PBS + 2% goat-serum (PBS-GS) overnight at 4°C. Cells were washed 3× for 5 min each with PBS-GS, then incubated with FITC anti-mouse IgG (Vector, Burlingame, CA), Texas Red-phalloidin (3.3 U/ml) (Molecular Probes, Eugene, OR), and DAPI (2 ng/ml) (Molecular Probes) for 2 h at 37°C. Cells were washed 3× for 5 min each with PBS-GS. Coverslips were mounted in glycerol and scored for the colocalization of DAPI-labeled *L. monocytogenes* with F-actin in iNOS-positive or -negative cells. Digital micrographs were taken using a Spot II cooled charge-coupled device camera (Diagnostic, Madison Heights, MI) on a Zeiss Axioplan II (Carl Zeiss, Thornwood, NY).

Pinocytosis in macrophages

Cells were plated at $2–3 \times 10^5$ cells per well in 24-well plates and incubated overnight in experimental treatments. After washing 3× with warm RB for 15 min, they were incubated with 0.5 mg/ml lucifer yellow CH (Molecular Probes) in warm RB for various times, washed 2× for 5 min each in successive 2 × 1 L beakers of cold PBS + 0.1% BSA, 1 L beaker of cold PBS, then lysed in 0.5 ml of lysis buffer (0.1% Triton X-100, 50 mM Tris, pH 8.5). Fluorescence of 0.4 ml lysate with 0.75 ml lysis buffer was measured in a spectrofluorometer using excitation 430 nm and emission 540 nm. Concentrations of lucifer yellow were determined using defined concentrations of lucifer yellow in lysis buffer. Protein per well was measured using the biscinchoninic acid protein assay (Pierce, Rockford, IL).

Measurement of macropinosome and phagosome progression

To measure the rate at which macropinosomes and phagosomes colocalize with LAMP-1, macrophages on 13-mm coverslips treated overnight were washed 3× with RB, then were incubated for 2 min with 1 mg/ml fixable fluorescein dextran, M^r 10,000 (FDx10f; Molecular Probes) plus 3,000 U/ml recombinant macrophage-colony-stimulating factor (rM-CSF; Genetics Institute, Cambridge, MA) or 3 min with 1 mg/ml FDx10f plus 1.0×10^7 opsonized sRBC. After washing 3× with RB, cells were incubated for various times in RB. Cells were fixed with a modified paraformaldehyde-lysine-periodate fixative ([20], G-PLP: 20 mM MES, 70 mM NaCl, 5 mM KCl, 70 mM Lysine-HCl, 5 mM $MgCl_2$, 2mM EGTA, 10 mM $NaIO_4$, 4.5% sucrose, 3.7% paraformaldehyde, pH 7.5) for 45 min at 37°C, then washed 3× for 5 min with 20 mM Tris-HCl, 150 mM NaCl, 4.5% sucrose, pH 7.2, supplemented with 2% goat serum (TBS-GS). Immunofluorescence was performed by incubating cells with rat anti-LAMP-1 antibody (Developmental Studies Hybridoma Bank, Iowa City, IA) for 1 h at 37°C. Cells were washed 3× for 5 min with TBS-GS, then incubated with Texas Red-labeled anti-rat IgG (Vector) for 1 h at 37°C. Cells were prepared for microscopy as described above. FDx10f-labeled macropinosomes and phagosomes were scored positive when they were completely labeled by LAMP-1.

To determine the rate of macropinosome fusion with lysosomes, macrophages on 13-mm coverslips were exposed to treatments overnight, then were incubated 30 min in DME-10F containing 0.5 mg/ml Texas Red Dextran, M^r 10,000 (TRDx10; Molecular Probes) to label endosomes. Cells were then

incubated for 1 h in DME-10F to redistribute TRDx10 into lysosomes. Cells were washed 3× with RB and pulsed for 2 min with 1 mg/ml FDx10 and 3,000 U/ml M-CSF. Cells were rapidly washed 3× and incubated in RB for various times before fixation with G-PLP fixative for 45 min at 37°C and preparation for microscopy, as described above. FDx10-labeled macropinosomes were located and scored for complete colocalization with TRDx10.

To assess the rate of macropinosome formation, macrophages were incubated with FDx10 (1 mg/ml) plus M-CSF (3,000 U/ml) in RB for various times. Cells were quickly washed then fixed with G-PLP fixative for 45 min at 37°C, rinsed 3× for 5 min in TBS-GS, prepared for microscopy, then scored for the presence of FDx10-labeled macropinosomes.

Measurement of macropinosome pH

Macropinosome pH was measured by quantitative fluorescence microscopy of FDx3-labeled organelles. To measure the pH in macropinosomes, macrophages on coverslips were washed 3× and mounted in a temperature-controlled stage at 37°C. Cells were pulsed with 0.75 mg/ml fluorescein dextran, M^r 3,000 (FDx3; Molecular Probes) and 3,000 U/ml M-CSF in warm RB for 1.5 min, then washed several times over 2.5 min in warm RB. Time-lapse images were acquired by phase-contrast and fluorescence microscopy, with excitation of 485 and 440 nm and emission of 520 nm on a Zeiss IM-35 inverted microscope (Carl Zeiss, Thornwood, NY). Images were analyzed with Metamorph image analysis software (Universal, West Chester, PA). The 485-nm image was thresholded to select the vacuole of interest, then a mask was created to select the identical area in the 440-nm image. The pH of the vacuole was calculated using a 485:440 nm ratio of the average vacuole intensity calibrated to vacuoles incubated in 10 μM nigericin (Molecular Probes) in isotonic potassium buffers of known pH (130 mM KCl, 1 mM $MgCl_2$, 15 mM Hepes, 15 mM MES, 0.02% sodium azide) [11].

Statistical analyses

Student's two-tailed *t*-test was applied to data from quantitative measurements, comparing data from nonactivated macrophages to that from LPS-, IFN-γ-, or LPS plus IFN-γ-treated macrophages. Figures show mean and standard error of the mean from all experiments.

RESULTS

Activation of bone marrow-derived macrophages

Bone marrow-derived macrophages incubated overnight in LPS and IFN-γ were activated by several measures. Production of nitrite increased after treatment with either stimulant and increased dramatically after exposure to both IFN-γ and LPS (**Fig. 1A**). The increases in nitrite reflected nitric oxide production in that its accumulation could be inhibited by 1 mM L-NMMA, a competitive inhibitor of iNOS [21]. Increases in cellular iNOS were indicated by westerns of macrophage lysates and by immunofluorescence localization of iNOS (data not shown). Independent measures of nitric oxide production, using fluorescent sensors of nitric oxide, also indicated increased nitric oxide production by activated macrophages [22]. Superoxide production after stimulation with phorbol myristate acetate was also increased in the activated macrophages (data not shown).

Macrophages activated with IFN-γ plus LPS inhibited intracellular growth of *L. monocytogenes*. The number of bacteria per macrophage increased significantly more in nonactivated than activated macrophages (Fig. 1B). The inhibition appeared to occur by prevention of bacterial escape from phagosomes, because the percentage of bacteria with associated F-actin, a measure of movement into the cytosolic space [19], was considerably reduced in the activated macrophages (Fig. 1C).

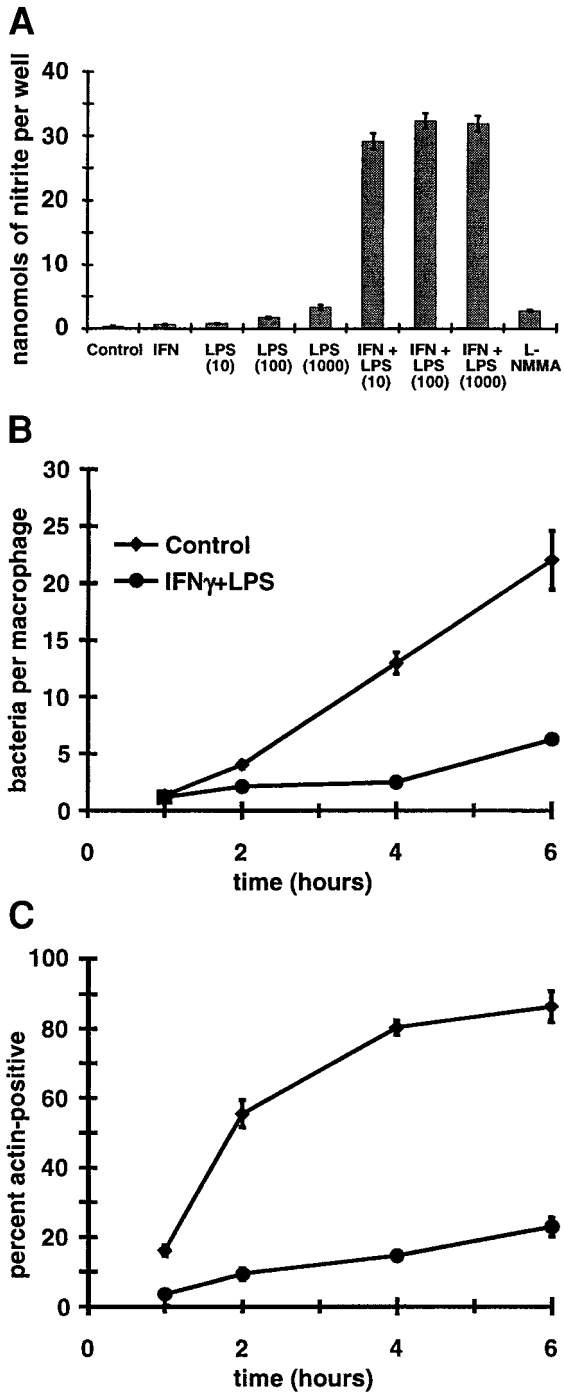

Fig. 1. Measures of macrophage activation. (A) Nitrite production by activated macrophages. Macrophage cultures were incubated 24 h in LPS (10–1,000 ng/ml) and/or IFN-γ (100 U/ml), then culture supernatents were measured for content of nitrite ($n > 11$). The right-most bar represents nitrite production after treatment with 1 mM N^G-monomethyl-L-arginine (L-NMMA) plus IFN-γ and 100 ng/ml LPS and indicates that the measured nitrite reflected nitric oxide production ($n = 3$). (B, C) Listericidal activities of activated macrophages. Macrophages on coverslips were infected with *L. monocytogenes* for 30 min, washed, and incubated for 0.5–5.5 h in medium with gentamicin. At the indicated times, cells were fixed and stained with DAPI and Texas Red-labeled phalloidin to determine (B) the number of bacteria per infected macrophage and (C) the percentage of bacteria containing associated F-actin. Macrophages activated with LPS plus IFN-γ inhibited both bacterial replication and the delivery into the cytosol. Data for activated macrophages differed significantly from control macrophages at 2, 4, and 6 h ($P < 0.04$; $n = 3$).

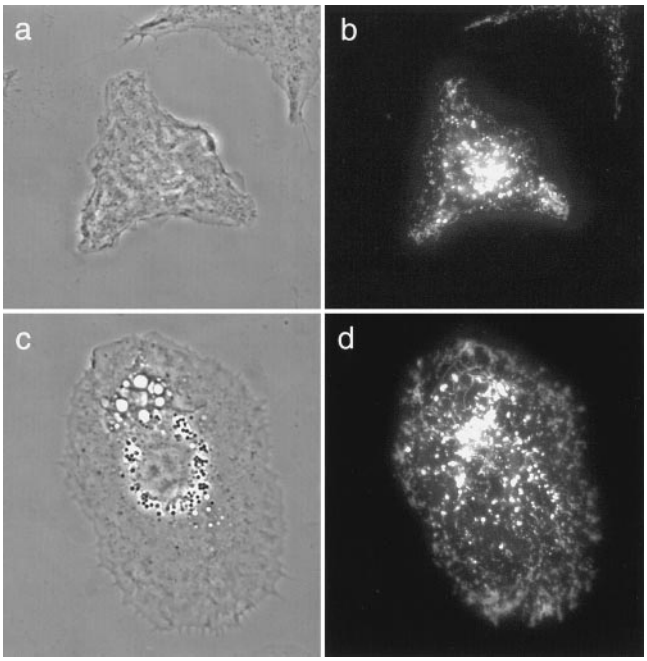

Fig. 2. Morphology of endocytic compartments in macrophages. Macrophages were activated by overnight incubation with IFN-γ and LPS (100 ng/ml). Activated (c, d) and nonactivated (a, b) macrophages were then pulse-labeled by endocytosis of FDx10 (30 min, followed by 60-min chase) and viewed by phase-contrast (a, c) and fluorescence (b, d) microscopy. Tubular and spherical lysosomes, labeled by endocytosis of fluorescein dextran, were evident in both activated and nonactivated macrophages. Activated macrophages contained prominent phase-dense perinuclear granules that were not labeled with the endocytic tracer.

Morphological changes accompanying activation

Macrophages activated with LPS and IFN-γ were a mixture of well-spread and rounded cells, all of which were generally larger than nonactivated macrophages. Time-lapse video microscopy revealed active ruffling and the occasional formation of phase-bright macropinosomes (data not shown). Vacuolar compartments labeled by pinocytosis of fluorescein dextran appeared essentially similar to those of nonactivated macrophages, consisting of small vesicles and tubular lysosomes that extended radially from the perinuclear region (**Fig. 2**). A notable difference between the two kinds of macrophage was the abundance in activated macrophages of phase-dense spherical granules (Fig. 2), which were either absent in nonactivated macrophages or, when present, were smaller than those of activated macrophages. The granules were also abundant after exposure with LPS only and, to a lesser extent, after exposure to IFN-γ. They appeared to be lipid granules because they could not be labeled with any of a variety of endocytic tracers and they were readily labeled with Nile Red, a stain for neutral lipids (data not shown).

Inhibition of pinocytosis

Constitutive pinocytosis, measured by the accumulation of lucifer yellow in populations of macrophages, was decreased after activation with IFN-γ, LPS, or both (**Fig. 3A**). The decreased accumulation apparently resulted from decreases in the rate and extent of pinosome formation, as measurements of efflux from cells preloaded with lucifer yellow showed no significant differences between activated and nonactivated macrophages (data not shown). Previous work determined that lucifer yellow and FDx10 are both internalized by fluid-phase pinocytosis in macrophages [4, 23], so their rates of accumulation and efflux can be taken as indicators of fluid solute flux independent of adsorptive or receptor-mediated components. Lucifer yellow was used to measure pinocytosis by populations of cells, because methods for measuring it in lysates are more sensitive than those for fluorescein-dextrans.

For morphological studies, however, in which ≥2 fluorophores must sometimes be compared in single cells, FDx10 is a preferable label for pinosomes. To compare rates of pinosome formation, macrophages were pulsed with FDx10 plus M-CSF

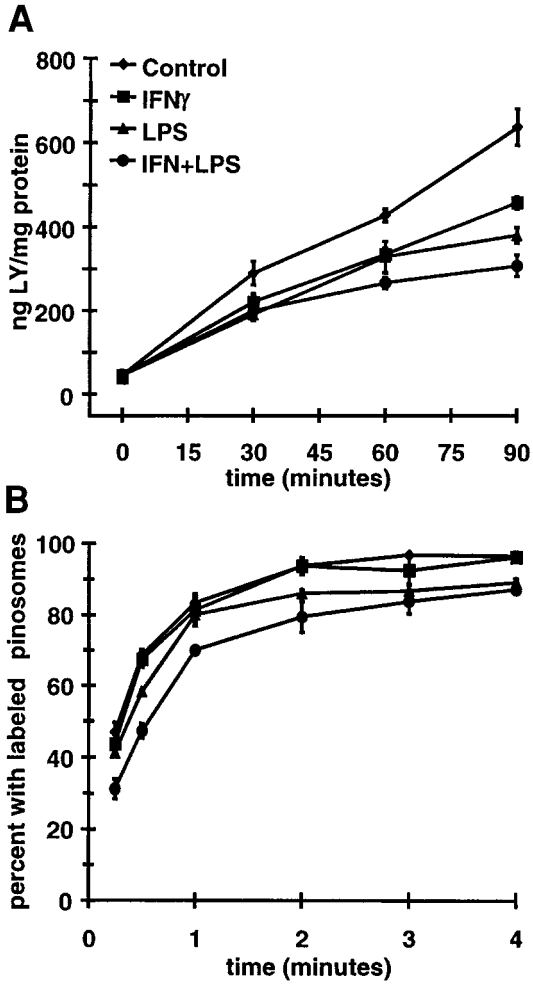

Fig. 3. Decreased pinocytosis in activated macrophages. (A) Macrophages incubated overnight in IFN-γ, LPS (100 ng/ml), neither, or both were incubated with 0.5 mg/ml lucifer yellow in RB for the indicated times before washing and lysing to measure cellular pinocytic accumulation. Macrophages activated with IFN-γ, LPS, or both showed significantly lower rates of pinocytosis than nonactivated controls ($P < 0.06$; $n = 8$). (B) Variously activated macrophages were incubated for the indicated times in RB containing FDx10 and M-CSF (1,000 U/ml), then the fraction of cells containing fluorescein-labeled macropinosomes was determined. Each time point represents the mean and SE of three experiments, in each of which 100 cells were scored for the presence of labeled macropinosomes. Nearly all macrophages activated with IFN-γ plus LPS formed macropinosomes, but they did so more slowly than the nonactivated macrophages ($P < 0.05$).

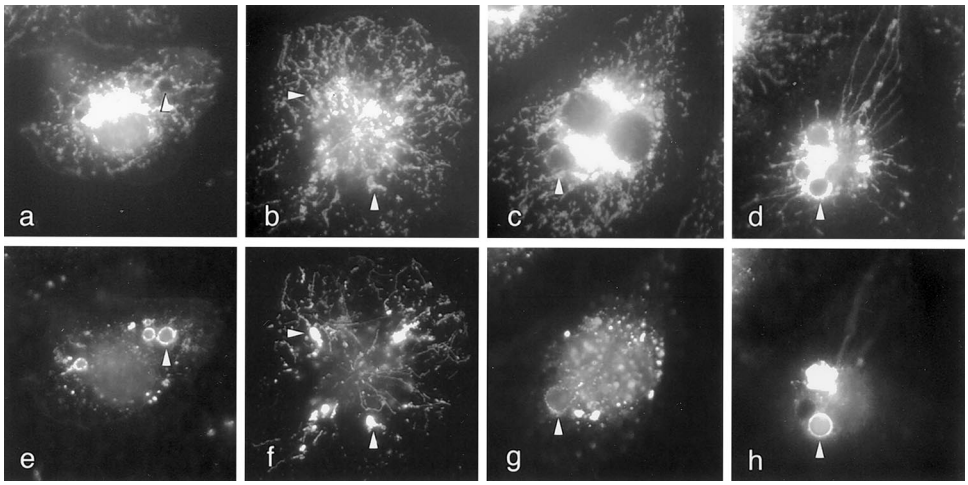

Fig. 4. Macropinosome and phagosome fusion with lysosomes. Macrophage lysosomes were labeled by endocytosis of TRDx10, then macropinosomes or phagosomes were pulse-labeled with FDx10 plus M-CSF (1,000 U/ml). Cells were then washed and chased for 5–20 min before fixing and scoring for presence of Texas Red in fluorescein-positive macropinosomes or phagosomes. The upper row of panels (a–d) shows TRDx10 images and the lower row (e–h) shows corresponding fluorescein dextran images. Arrowheads show an unfused macropinosome (panels a, e), fused macropinosomes (b, f), an unfused phagosome (c, g), and a fused phagosome (d, h). Cells labeled for immunofluorescence of LAMP-1 showed patterns of fluorescence similar to those of cells labeled by endocytosis of TRDx10.

for various intervals, then the fraction of cells containing labeled macropinosomes was determined (Fig. 3B). Activated macrophages formed macropinosomes more slowly, and a small percentage of the cells did not produce macropinosomes at all. Figure 3B indicates that nearly all activated macrophages made pinosomes, which is consistent with the interpretation that all cells have decreased rates of pinocytosis. The relative effects of M-CSF on pinocytosis of activated and nonactivated macrophages were not measured.

Delayed fusion with lysosomes

Activated macrophages also showed delayed progression of macropinosomes and phagosomes to the lysosomal compartment. Rates of progression were determined by measuring, at various times after their formation, the fraction of pulse-labeled macropinosomes formed in the presence of M-CSF or phagosomes that contained markers of late endosomes or lysosomes. Lysosome-associated membrane protein-1 (LAMP-1) served as a marker of late endosomes and lysosomes, and TRDx10, loaded by pinocytosis and a 60-min chase, served as a marker for lysosomes. Consequently, labeling for LAMP-1 allows measurement of pinosome progression to late endosomes, and pulse-chase-labeling with TRDx10 shows progression to later compartments [24]. Examples of fused and unfused macropinosomes and phagosomes are shown in **Figure 4**. Immunofluorescence labeling for LAMP-1 appeared very similar to the images of TRDx10-loaded late endosomes and lysosomes (data not shown).

Rates of fusion were discernable from the fractions of FDx-labeled organelles that contained Texas Red, measured at various chase times after the FDx pulse. As in earlier studies [24], macropinosomes of nonactivated macrophages acquired LAMP-1 (i.e., lgp-A) several minutes earlier than TRDx10 from preloaded lysosomes. Macropinosomes of activated macrophages acquired both LAMP-1 and TRDx10 more slowly than those of nonactivated macrophages. In cells activated with both IFN-γ and LPS, the chase time required to label half of the macropinosomes was 6 min longer than that required to label half the pinosomes of nonactivated cells (**Fig. 5A, B**). Macrophages activated with IFN-γ or LPS alone showed intermediate progression rates, with LPS generally slowing things more than IFN-γ. Macropinosome progression was difficult to assess after a 20 min chase, as nearly all macropinosomes had shrunken completely by that time. In all macrophages, phagosomes containing IgG-opsonized sheep erythrocytes acquired LAMP-1 nearly as quickly as macropinosomes did; and like macropinosome progression, the phagosomes of activated macrophages acquired LAMP-1 more slowly than the phagosomes of nonactivated macrophages (Fig. 5C).

Unchanged rates of macropinosome acidification

The delayed progression of macropinosomes and phagosomes, and the slowing of pinocytosis, suggested that endocytic organelle acidification may also be slowed in activated macrophages. To measure rates of acidification, macrophages were pulse-labeled with FDx3 in the presence of M-CSF, a stimulant of macropinocytosis, then the pH of individually labeled macropinosomes was measured by fluorescence microscopy at various intervals after the pulse. A population average for macropinosome acidification was obtained by ratiometric measurements of pH. The cumulative data indicated that macropinosome acidification occurred at the same rapid rate in activated and nonactivated macrophages. A pH of 5.1 was reached within 10 min of macropinosome formation, and this pH was maintained for many hours (**Fig. 6**). Activated and nonactivated macrophages maintained the same resting pH in their lysosomal compartments, which had been labeled by short pulses of FDx3 followed by chase periods of 24 h (Fig. 6).

Together, these data indicate that activation results in slower delivery of pinocytosed and phagocytosed materials to lyso-

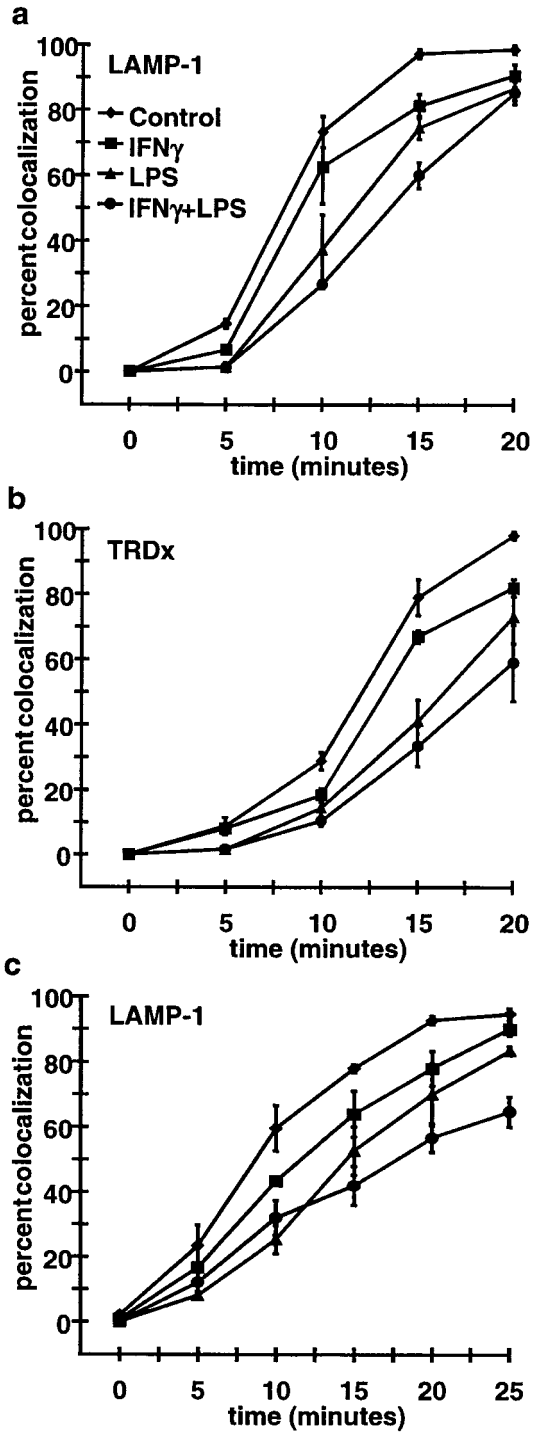

Fig. 5. Delayed fusion of macropinosomes and phagosomes with lysosomes in activated macrophages. Macrophages were cultured overnight in IFN-γ and/or LPS, as indicated. (a) Macropinosomes were pulse-labeled for 2 min with FDx10 plus M-CSF (1,000 U/ml), then were chased for the indicated times before fixing and staining for localization of LAMP-1. FDx10-positive pinosomes were scored for the presence of LAMP-1. Values for LPS and LPS plus IFN-γ differed significantly from the control group ($P < 0.04$; $n = 3$). (b) Lysosomes were labeled by incubation with TRDx, followed by a 60-min chase in unlabeled medium. Macropinosomes were pulse-labeled with FDx10 plus M-CSF as in panel A, and FDx10-positive pinosomes were scored for the presence of TRDx. Values for IFN-γ, LPS, and LPS plus IFN-γ differed significantly from the control group ($P < 0.04$; $n = 3$–5), except for IFN-γ-treated cells at 5 and 15 min. (c) Phagosomes were pulse-labeled with FDx10 for 3 min during the ingestion of IgG-opsonized sheep erythrocytes. After chase periods for the indicated times, cells were fixed and stained to localize LAMP-1 in FDx10-positive phagosomes. Values for LPS and LPS plus IFN-γ were significantly different than controls at times 15 and 25 min ($P < 0.03$; $n = 3$). Each time point represents the mean and SE of three experiments, in each of which 25 labeled organelles were scored.

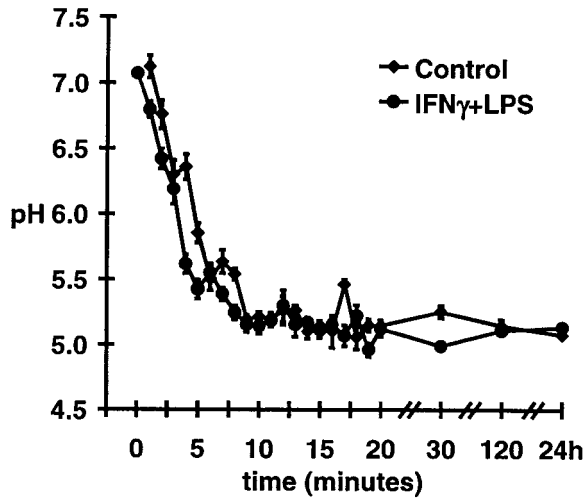

Fig. 6. Macropinosome acidification in macrophages. Macrophages on coverslips were labeled by a 1.5-min pulse of FDx3 plus M-CSF followed by a 2.5-min wash, then the pH of individual macropinosomes was measured at the indicated intervals after the wash. Data are cumulative measurements. At no time point did the pH for activated macrophages differ significantly from the control group. For times 0–20 min, $n = 6$–48; for 2 h, $n = 148$ and 70; for 24 h, $n = 170$ and 98.

somes but equally rapid acidification of endocytic organelles (**Fig. 7**). In effect, this produces an enlarging of the prelysosomal acidic compartment, one which may be optimal for microbicidal chemistries.

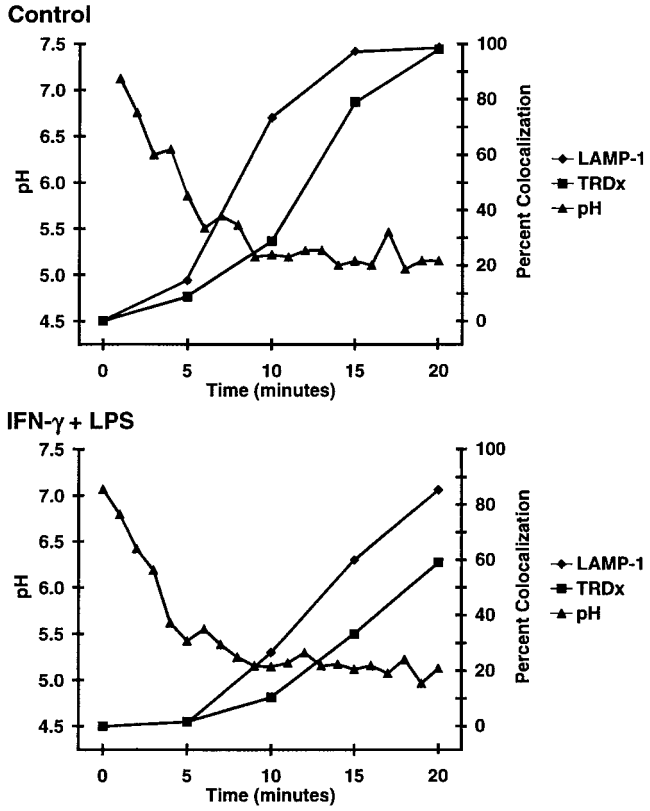

Fig. 7. Rapid acidification and delayed progression of macropinosomes in activated macrophages activated with LPS plus IFN-γ. Data from Figs. 5a, b and 6 are combined to indicate the essential differences in organelle dynamics. Activated macrophages contain an expanded nonlysosomal endocytic compartment.

DISCUSSION

These studies demonstrate that macrophages activated with IFN-γ and LPS slow their endocytosis and membrane trafficking relative to nonactivated cells. Activation increased some activities, such as production of nitric oxide and resistance to intracellular growth of *L. monocytogenes*, yet decreased organelle dynamics generally. This slowing could be a counterproductive consequence of producing toxic microbicidal compounds, or it could be a contributing element of the cell's microbicidal functions.

With exposure to LPS and IFN-γ, bone marrow-derived macrophages acquire many features of activated primary macrophages [6]. Consistent with previous studies, exposure of bone marrow-derived macrophages to IFN-γ and LPS increased production of nitric oxide [25]. Separate studies determined that this protocol also increased superoxide production in response to phorbol ester treatment (data not shown). These activated macrophages were also more resistant to infection by *L. monocytogenes*, although they were not as fully microbicidal as peritoneal macrophages treated with IFN-γ [10] (A. W. T., data not shown). Different protocols for obtaining and activating macrophages result in different levels of listericidal activity in macrophages [26]. The mechanisms underlying this heterogeneity in responsiveness are not known but are likely to be related to the fact that activation itself is not a singular differentiation event. In some cases, IFN-γ alone is sufficient to increase listericidal activities [10], whereas in other cases, macrophages are only listericidal after exposure to both IFN-γ and LPS [27]. Bone marrow-derived macrophages were selected for these studies because exposure to IFN-γ and LPS increases measurably their resistance to *L. monocytogenes* and their expression of biochemical markers of activation, and because the flattened morphologies of these cells render them optimal for quantitative microscopic study.

The morphologies of activated macrophages were essentially as described previously, with one notable difference in the properties of the abundant phase-dense granules. Earlier studies characterized the phase-dense granules in LPS-activated macrophages as lysosomes [9]. However, the phase-dense granules seen here were apparently not part of the endocytic compartment, at least as defined by labeling with fluorescent tracers. Our preliminary studies indicate that they are lipid granules (J. A. S., data not shown).

The slowing of membrane trafficking observed in activated macrophages was measurable at several levels. Pinosomes formed more slowly, as did phagosomes (data not shown). Rates of fusion between pinosomes and lysosomes, and between phagosomes and lysosomes, were also reduced. These changes were not a result of decreased viability, as >95% of the activated macrophages continued to exclude propidium iodide (data not shown). The lower rates of phagosome-lysosome fusion contrast with the results of Kielian and Cohn [28], who observed increased rates of phagosome-lysosome fusion in macrophages elicited by peritoneal injection of *Trypanosoma cruzi*, *Toxoplasma gondii*, or proteose peptone. The different results may be a result of differences in methods of activation or of differences in the assays for phagosome-lysosome fusion.

The conclusion of this study, that endocytosis is slowed in activated macrophages, is not fundamentally at odds with earlier studies that reported increased pinocytosis in activated macrophages. Methodological differences underlie the different conclusions. An earlier report of increased pinocytosis in thioglycollate-elicited macrophages was evidently not describing fluid-phase pinocytosis exclusive of receptor-mediated endocytosis [13]. That study measured pinocytosis using HRP, a probe which was later shown to enter macrophages by both fluid-phase pinocytosis and mannose receptor-mediated endocytosis [29] and to stimulate fluid-phase pinocytosis itself [30]. Increased mannose-receptor-mediated endocytosis in thioglycollate-elicited macrophages could explain the measured increases of HRP accumulation. In another study, in which LPS increased rates of pinocytosis in bone marrow-derived macrophages [14], pinocytosis was measured immediately after LPS addition, rather than much later, and the data therefore would not reflect pinocytosis in activated macrophages. The reduced rates of trafficking described here are consistent with recent observations of Montaner et al. [15], in which prolonged exposure to IFN-γ led to a general reduction in rates of pinocytosis in human monocytes. After correcting for mannose-receptor-mediated endocytosis, they showed that pinocytic accumulation of HRP by IFN-γ-activated monocytes was reduced relative to nonactivated control monocytes.

Pinocytic influx was slowed without attendant decreases in fluid-phase recycling. Various effects of cell stimulation on rates of influx and efflux have been noted previously [14]. It has been proposed that such changes can occur without net redistribution of cell membranes by changing the size ratios (i.e., average diameters) of influx and efflux vesicles [4].

The activated macrophages exhibited a decrease in membrane trafficking without a decrease in rates of vesicle acidification. This indicates that the H^+-ATPase, that acidifies the vacuolar compartment, localizes to early endosomes in both activated and nonactivated macrophages.

The aggregate effect of activation with IFN-γ and LPS was a prolonged residence of particles and macromolecules in acidic nonlysosomal compartments (Fig. 7). Macropinosomes acidified rapidly but acquired LAMP-1 and lysosomal content markers slowly. This alteration in the dynamics of the compartments created a novel microenvironment without creating a new organelle. This compartment may serve novel functions peculiar to the activated macrophage. An acidic compartment deficient in acid hydrolases could facilitate peptide loading onto MHC class II molecules, or it could optimize antimicrobial chemistries involving reactive oxygen or nitrogen species.

How important is a 6-min delay in endocytic vesicle progression to the microbicidal activities of macrophages? This will most likely depend on which microbe is considered. For the slow-growing intracellular parasite *Mycobacterium tuberculosis*, changes in rates of membrane trafficking may be of less consequence than biochemical changes that would impair intracellular growth. Phagosomes containing *M. tuberculosis* do not fuse with lysosomes in nonactivated macrophages, but activation of macrophages with IFN-γ and LPS increases delivery of *M. tuberculosis*-containing phagosomes into the lysosomal compartment [31]. This indicates that activation causes a significant change in the dynamics of *M. tuberculosis*-con-

taining phagosomes specifically. For *L. monocytogenes*, however, which escapes from phagosomes of nonactivated macrophages shortly after phagocytosis [11], changes in early rates of phagosome progression to lysosomes could affect the ability of bacteria to escape into cytoplasm. Activation inhibits the ability of *L. monocytogenes* to escape from the phagosome [10]. Slowed phagosome maturation in activated macrophages of the magnitude reported here could alter the nature of the enclosing membrane so as to limit the ability of *L. monocytogenes* hemolysin to perforate that membrane.

ACKNOWLEDGMENTS

We thank Dr. Kenneth Christensen for technical advice and Nikhil Joshi for assistance. We gratefully acknowledge gifts of M-CSF from Genetics Institute, Cambridge, MA, and sheep blood from the Reproductive Science Program at the University of Michigan. Supported by NIH Grant AI 35950 to J. A. S.

REFERENCES

1. Kaufmann, S. H. E. (1999) Immunity to intracellular bacteria. In *Fundamental Immunology*, 4th ed. (W. E. Paul, ed.) New York, Lippincott-Raven, 1335–1371.
2. Pacelli, R., Wink, D. A., Cook, J. A., Krishna, M. C., DeGraff, W., Friedman, N., Tsokos, M., Samuni, A., Mitchell, J. B. (1995) Nitric oxide potentiates hydrogen peroxide-induced killing of *Escherichia coli*. J. Exp. Med. 182, 1469–1479.
3. Germain, R. N. (1994) MHC-dependent antigen processing and peptide presentation: providing ligands for T lymphocyte activation. Cell 76, 287–299.
4. Swanson, J. A. (1989) Phorbol esters stimulate macropinocytosis and solute flow through macrophages. J. Cell Sci. 94, 135–142.
5. Mackaness, G. B. (1962) Cellular resistance to infection. J. Exp. Med. 116, 381–406.
6. Adams, D. O., Hamilton, T. A. (1987) Molecular transductional mechanisms by which IFNγ and other signals regulate macrophage development. Immunol. Rev. 97, 5–27.
7. Nacy, C. A., Meltzer, M. S. (1991) T-cell-mediated activation of macrophages. Curr. Opin. Immunol. 3, 330–335.
8. MacMicking, J., Xie, Q.-W., Nathan, C. (1997) Nitric oxide and macrophage function. Annu. Rev. Immunol. 15, 323–350.
9. Cohn, Z. A., Benson, B. (1965) The differentiation of mononuclear phagocytes: morphology, cytochemistry, and biochemistry. J. Exp. Med. 121, 153–170.
10. Portnoy, D. A., Schreiber, R. D., Connelly, P., Tilney, L. G. (1989) γ-Interferon limits access of *Listeria monocytogenes* to the macrophage cytoplasm. J. Exp. Med. 170, 2141–2146.
11. Beauregard, K. E., Lee, K.-D., Collier, R. J., Swanson, J. A. (1997) pH-dependent perforation of macrophage phagosomes by listeriolysin O from *Listeria monocytogenes*. J. Exp. Med. 186, 1159–1163.
12. Sallusto, F., Cella, M., Danieli, C., Lanzavecchia, A. (1995) Dendritic cells use macropinocytosis and the mannose receptor to concentrate macromolecules in the major histocompatibility complex class II compartment: downregulation by cytokines and bacterial products. J. Exp. Med. 182, 389–400.
13. Edelson, P. J., Zweibel, R., Cohn, Z. A. (1975) The pinocytic rate of activated macrophages. J. Exp. Med. 142, 1150–1164.
14. Knight, K. R., Vairo, G., Hamilton, J. A. (1992) Regulation of pinocytosis in murine macrophages by colony-stimulating factors and other agents. J. Leukoc. Biol. 51, 350–359.
15. Montaner, L. J., da Silva, R. P., Sun, J., Sutterwala, S., Hollinshead, M., Vaux, D., Gordon, S. (1999) Type 1 and type 2 cytokine regulation of macrophage endocytosis: differential activation by IL4/IL13 as opposed to IFNγ or IL-10. J. Immunol. 162, 4606–4613.
16. Adams, D. O., Hamilton, T. A. (1984) The cell biology of macrophage activation. Annu. Rev. Immunol. 2, 283–318.
17. Racoosin, E. L., Swanson, J. A. (1989) Macrophage colony stimulating factor (rM-CSF) stimulates pinocytosis in bone marrow-derived macrophages. J. Exp. Med. 170, 1635–1648.
18. Granger, D. L., Taintor, R. R., Boockvar, K. S., Hibbs, J. B. (1996) Measurement of nitrate and nitrite in biological samples using nitrate reductase and Greiss reaction. Meth. Enzymol. 268, 142–151.
19. Jones, S., Portnoy, D. A. (1994) Intracellular growth of bacteria. Meth. Enzymol. 236, 463–467.
20. McLean, I. W., Nakane, P. K. (1974) Periodate-lysine-paraformaldehyde fixative: a new fixative for immunoelectron microscopy. J. Histochem. Cytochem. 22, 1077–1083.
21. Bogle, R. G., MacAllister, R. J., Whitley, G. S., Vallance, P. (1995) Induction of NG-monomethyl-L-arginine uptake: a mechanism for differential inhibition of NO synthesis. Am. J. Physiol. 269, C750.
22. Barker, S. L. R., Kopelman, R., Meyer, T. E., Cusanovich, M. A. (1998) Fiber optic nitric oxide selective biosensors and nanosensors. Anal. Chem. 70, 971–976.
23. Berthiaume, E. P., Medina, C., Swanson, J. A. (1995) Molecular size-fractionation during endocytosis in macrophages. J. Cell Biol. 129, 989–998.
24. Racoosin, E. L., Swanson, J. A. (1993) Macropinosome maturation and fusion with tubular lysosomes in macrophages. J. Cell Biol. 121, 1011–1020.
25. Appelberg, R., Orme, I. M., Pinto de Sousa, M. I., Silva, M. T. (1992) *In vitro* effects of interleukin-4 and interferon-γ-induced macrophage activation. Immunology 76, 553–559.
26. Fleming, S. D., Campbell, P. A. (1997) Some macrophages kill *Listeria monocytogenes* while others do not. Immunol. Rev. 158, 69–77.
27. Higgenbotham, J. N., Lin, T. L., Pruett, S. B. (1992) Effect of macrophage activation on killing of *Listeria monocytogenes*: roles of reactive oxygen or nitrogen intermediates, rate of phagocytosis, and retention of bacteria in endosomes. Clin. Exp. Immunol. 88, 492–498.
28. Kielian, M. C., Cohn, Z. A. (1981) Modulation of phagosome-lysosome fusion in mouse macrophages. J. Exp. Med. 153, 1015–1020.
29. Sung, S.-S. J., Nelson, R. S., Silverstein, S. C. (1983) The role of the mannose/N-acetylglucosamine receptor in the pinocytosis of horseradish peroxidase by mouse peritoneal macrophages. J. Cell Physiol. 116, 21–25.
30. Swanson, J. A., Yirinec, B. D., Silverstein, S. C. (1985) Phorbol esters and horseradish peroxidase stimulate pinocytosis and redirect flow of pinocytosed fluid through macrophages. J. Cell Biol. 100, 851–859.
31. Schaible, U. E., Sturgill-Koszycki, S., Schlessinger, P. H., Russell, D. G. (1998) Cytokine activation leads to acidification and increases maturation of *Mycobacterium avium*-containing phagosomes in murine macrophages. J. Immunol. 160, 1290–1296.